Natural and Artificial Aging of Polypropylene–Polyethylene Copolymers

X. Colom,[1] J. Cañavate,[1] J. J. Suñol,[2] P. Pagès,[3] J. Saurina,[2] F. Carrasco[4]

[1] *Department of Chemical Engineering, Universitat Politècnica de Catalunya, C/Colom 1, E-08222 Terrassa, Spain*
[2] *Department of Physics, Universitat de Girona, Av. Luís Santaló s/n, E-17071 Girona, Spain*
[3] *Department of Materials Science, Universitat Politècnica de Catalunya, C/Colom 11, E-08222 Terrassa, Spain*
[4] *Department of Chemical Engineering, Universitat de Girona, Av. Luís Santaló s/n, E-17071 Girona, Spain*

Received 28 February 2002; accepted 3 June 2002

ABSTRACT: The degradation of polypropylene–polyethylene copolymers (which were used to make the seats for the Olympic stadium in Barcelona, Spain), in response to natural aging for 2.5 years and artificial aging for 5000 h in a xenon lamp chamber, was studied. The extent of the various photoreactions, including the formation of carbonyl groups, the scission of hydrocarbonated chains, the formation of free radicals in tertiary carbons, and the formation of nonsaturated bonds followed by branching and crosslinking, was analyzed by Fourier transform infrared spectrophotometry. Melting and thermal decomposition were studied by differential scanning calorimetry. In all cases, aging led to a loss of crystallinity. By scanning electron microscopy, it was possible to detect the formation of a porous material after melting crystallization, as well as the presence of micelle orientation. Finally, a comparison between natural and artificial aging effects showed differences, the samples exposed to weathering being modified to a greater extent than the artificially aged ones. © 2002 Wiley Periodicals, Inc. J Appl Polym Sci 87: 1685–1692, 2003

Key words: ageing; poly(propylene) (PP); polyethylene (PE); FT-IR; differential scanning calorimetry (DSC)

INTRODUCTION

It is known that exposing polymeric materials to environmental and artificial atmospheres changes their properties and external appearances with some modification of their surfaces. Several chemical reactions, induced by irradiation with sunlight, take place because of the chromophoric groups present in the polymer and the consequent ability of the polymer to absorb ultraviolet light Photoreactions are usually induced when polymer materials are damaged, causing embrittlement and color changes.[1–3] For the prevention of these phenomena, several methods have been developed. One of the most important is stabilizing the polymers with additives (i.e., antioxidants and light stabilizers).

To develop effective formulations, we must first know the causes and mechanism of the degradation. Fourier transform infrared (FTIR), differential scanning calorimetry (DSC), and scanning electron microscopy (SEM) are techniques used to evaluate the degradation process of polymeric materials. One of the earliest works performed with FTIR spectrophotometry was based on a study of PET films exposed to high temperatures.[4] More recently, several studies on the artificial aging of different polymers were carried out, and their effects were quantified by FTIR spectrophotometry and photoacoustic FTIR.[3,5–7]

In this article, we report on aging-induced changes in the structural and thermal properties of polypropylene (PP)–polyethylene (PE)-based copolymers that were used as seats in the Olympic stadium of Barcelona, Spain. The samples were exposed to natural aging by weather for 2.5 years and to artificial aging by exposure to radiation from a xenon lamp for 5000 h, which is considered to be equivalent to 2.5 years of environmental exposure.[8]

EXPERIMENTAL

The analyzed material was a PP-rich (~95 wt %) PP–PE copolymer manufactured by Repsol and marketed as PB 140. It was a block copolymer with short PE chains grafted to PP. The composition (95% PP) was chosen for its mechanical properties, that is, the high degree of toughness. Several additives were added to the base material. Table I shows a list of the various samples, which differed in the types and quantities of the additives employed.

The additives were antioxidants (Tinuvin 770, Irganox BZ15, Bioxid Kronos CL 2220, and Quimasorb 944) and colorants (blue Cromoftal A3R, red Cromoftal DPP-BO, violet Cinquasia R RT 891D, Iagacolor 10401, Byferrox 110, and Iagacolor 415).

Correspondence to: X. Colom (colomf@eq.upc.es).

Journal of Applied Polymer Science, Vol. 87, 1685–1692 (2003)

TABLE I
Description of the Additives Present in the Studied Copolymers

Sample	Additives
A	Tinuvin 770, Igamoz BZ15, Quimasorb 944, Cromoftal A3R, Bioxid Kronos CL 2220
B	Tinuvin 770, Quimasorb 944, Cromoftal DPP-BO, Cinquasia R RT 891D
C	Tinuvin 770 Igarnoz BZ15, Quimasorb 944, Iagacolor 10401 Bioxid Kronos CL 2220
D	Tinuvin 770, Quimasorb 944, Iagacolor 415, Byferrox 110

The coupled samples A–B and C–D were prepared with different combinations of coloring additives according to the main industrial process. Samples A and B were subjected to artificial aging performed in a xenon test 450 chamber, with a xenon arc lamp as the radiating light source for the simulation of natural aging. The artificial aging time was 5000 h (equivalent to 2.5 years of natural aging). The samples were labeled as A-5000 and B-5000, respectively. Samples C and D were aged under natural climatic conditions for 2.5 years and were labeled C-2.5 and D-2.5, respectively.

The structural changes and thermal properties of the PP–PE copolymers were measured with FTIR spectrophotometry and DSC techniques. A Nicolet 510M spectrometer with CsI optics was used to obtain the FTIR spectra, with a resolution of 2 cm^{-1} and with an average of 50 scans. Pellets were prepared by the dispersion of the surfaces of finely divided samples (3 mg) in a matrix of KBr (300 mg), followed by compression at 167 MPa.

To determine changes in the FTIR spectra, several authors[3,7,9] chose a particular band as a reference to avoid deviations between spectra produced by samples of different weights or thicknesses. The absorption related to this band is known as the reduced or compensated absorption. In this work, the spectral reference band chosen was at 2840 cm^{-1} and was due to methylene symmetric stretching vibrations.

The thermal behavior of the samples was analyzed with DSC. The measurements were made with a Mettler TA4000 thermoanalyzer coupled with a low-temperature (nitrogen coil) DSC 30 apparatus. The calibration of the temperatures and energies was made with standard samples of In, Pb, and Zn under the same conditions used in the sample analysis. The measurements were made with dry air as a purging gas at a flow rate of 20 mL/min. The heating rate was 10 K/min, a good compromise between the measurement rate and the endothermic melting peak resolution. The sample mass was about 2.5 mg, small enough to prevent the problems caused by heat- and mass-transfer limitations. Several experiments were performed to ensure the reproducibility of the results, with the samples heated to 600, 300, or 185°C.

The microstructures of the samples were characterized by SEM in a Zeiss DSM 960 A apparatus. The resolution was 3.5 nm, the acceleration voltage was 15 kV, and the working distance was 10–20 mm. The samples were sputtered previously with C with a K 550 Emitech instrument. The aim was to observe microstructural changes arising from the degradation phenomena related to the aging processes, as well as the effects of the thermal treatments applied to the material.

RESULTS AND DISCUSSION

We analyzed the characteristic spectral bands of the polymer that were more greatly modified during the aging process. The results are shown in Table II. The chemical groups related to these bands are carbonyl groups (1735 cm^{-1}), ether (1167 cm^{-1}), nonsaturated bonds (1650 cm^{-1}), methylene (1460 cm^{-1}), and methyl (1378 cm^{-1}). There are also three bands related to the structural characteristics: configuration isomerism and conformational order (812, 901, and 976

TABLE II
Variation of Reduced Absorbance Average Values of All Samples as a Function of Artificial Aging and Natural Aging

Wavenumber (cm^{-1})	Functional group	Reduced absorbance average values							
		A	A-5000	B	B-5000	C	C-2.5	D	D-2.5
1740	C═O	0.077	0.083	0.092	0.096	0.109	0.161	0.109	0.118
1735	(ester)	0.075	0.097	0.104	0.097	0.104	0.174	0.104	0.133
1720	C═O	0.059	0.090	0.083	0.096	0.088	0.169	0.088	0.106
1717	(ketone)	0.059	0.097	0.082	0.097	0.088	0.169	0.088	0.105
1167	C—O	0.206	0.212	0.203	0.200	0.250	0.291	0.268	0.276
1650	C═C	0.135	0.109	0.220	0.106	0.201	0.134	0.201	0.182
1460	—CH_2—	1.053	0.994	1.003	0.923	1.273	0.998	1.273	1.173
1378	—CH_3	1.174	1.072	1.117	1.106	1.354	1.146	1.354	1.262
976	Iso-PP	0.251	0.348	0.256	0.303	0.399	0.600	0.467	0.600
901	Iso-PP	0.067	0.085	0.066	0.079	0.082	0.132	0.091	0.132*
812	Iso-PP	0.067	0.108	0.070	0.091	0.091	0.140	0.098	0.140

This band moves to 912 cm^{-1}.

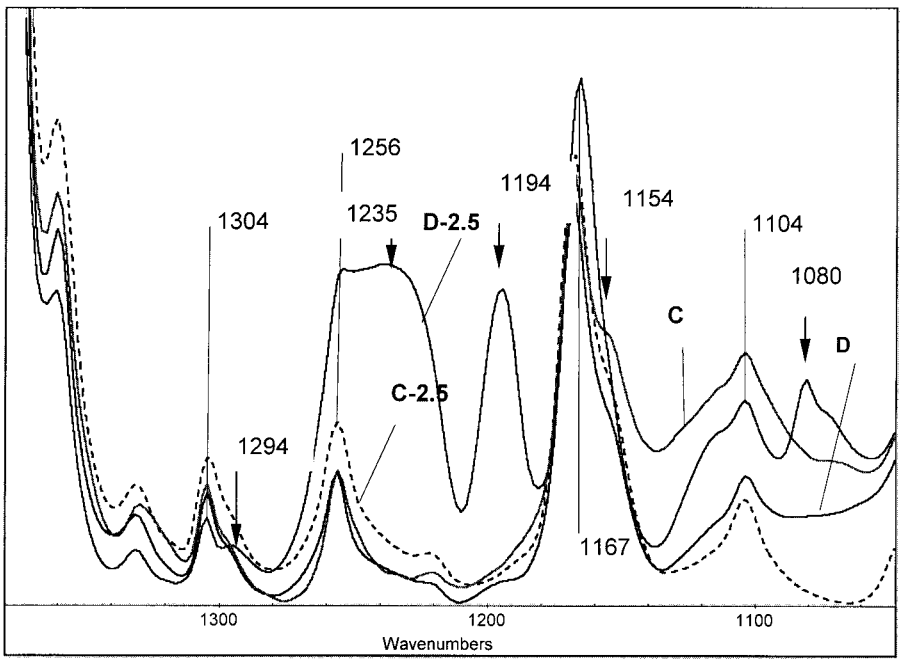

Figure 1 FTIR spectra of samples C and D exposed to natural aging in the spectral range 1025–1380 cm^{-1}.

cm^{-1}). The evolution of these latter bands allowed us to determine structural and configurational changes.

Study of natural aging by FTIR

Figure 1 shows the spectral range 1025–1380 cm^{-1} for samples C and D exposed to natural aging. The 1168-cm^{-1} band, associated with the C—O—C group, shows a tendency to increase in aged samples, suggesting the formation of ether groups. Moreover, the FTIR spectrum of sample D-2,5 has three bands at 1235, 1194, and 1080 cm^{-1} (marked by arrows) and two shoulders, one at 1294 cm^{-1} and another at 1154 cm^{-1} (marked by arrows), associated with transitions of the crystalline phase. These spectral differences between the aged and nonaged samples show that the crystallinity of sample D was more affected by the aging process. Sample C was less affected by aging, showing only small spectral changes (the 1235-cm^{-1} band and the shoulder at 1154 cm^{-1}).

Figure 2 shows the spectral range 750–1050 cm^{-1} corresponding to samples C and D not aged and naturally aged. The absorbance of the 812-, 976-, and 998-cm^{-1} bands, related to conformational and configurational changes, is higher in aged samples than in nonaged ones. Moreover, the presence of the bands marked by arrows makes it evident that some changes were produced. The spectral band at 901 cm^{-1} moved to 912 cm^{-1}, and this short shift was attributed to the background changes generated by conformational modifications. Likewise, a small shoulder appears at 941 cm^{-1}, and two peaks appear at 1015 and 1035 cm^{-1} (associated with the stretching vibrations of —C—O—C— and —C—O—H, respectively). Both peaks appear as a result of the oxidative process that originated during natural aging.

Study of artificial aging by FTIR

Samples A and B were subjected to artificial aging in the xenon test chamber for 5000 h. The spectra of aged and nonaged samples are shown in Figures 3 and 4. The changes detected in both materials (A and B) are very similar. Nevertheless, these changes are not as important as they are for the materials subjected to natural aging for 2.5 years (C and D).

The spectra corresponding to the samples artificially aged (A and B), illustrated in Figure 4, show that degradation phenomena are lower than in the previous case. In the artificially aged samples, only a slight increase in the band absorbances associated with the configuration order was detected. We can conclude, therefore, that exposure to weather leads to more aggressive degradation than that produced by exposure to the homogeneous conditions employed in the xenon test chamber in our study.

Comparison of natural and artificial aging by FTIR

A comparative study of both types of aging processes (natural and artificial) is shown in Figure 5. An increase of the ester and ketone groups (1735 and 1717 cm^{-1}) was detected. This increase was greater in the materials subjected to natural aging. Samples C were the most affected by carbonyl group formation.

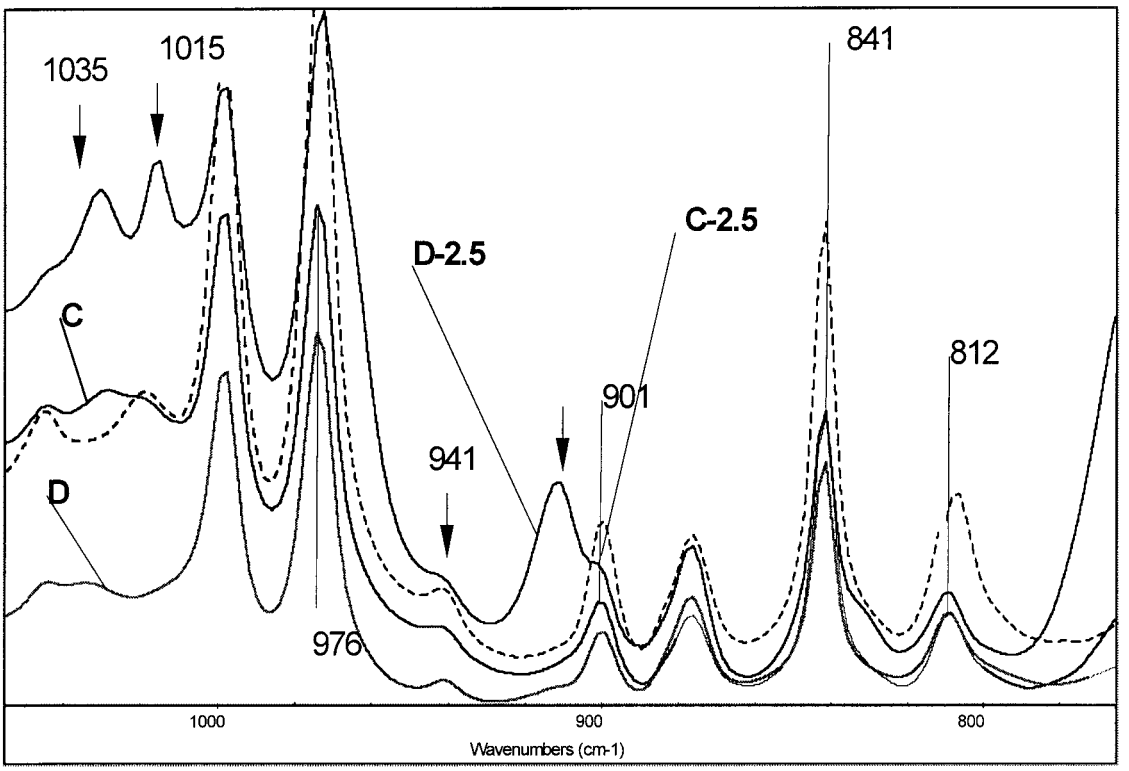

Figure 2 FTIR spectra of samples C and D exposed to natural aging in the spectral range 750–1050 cm^{-1}. Bands marked with arrows are related to large spectral changes.

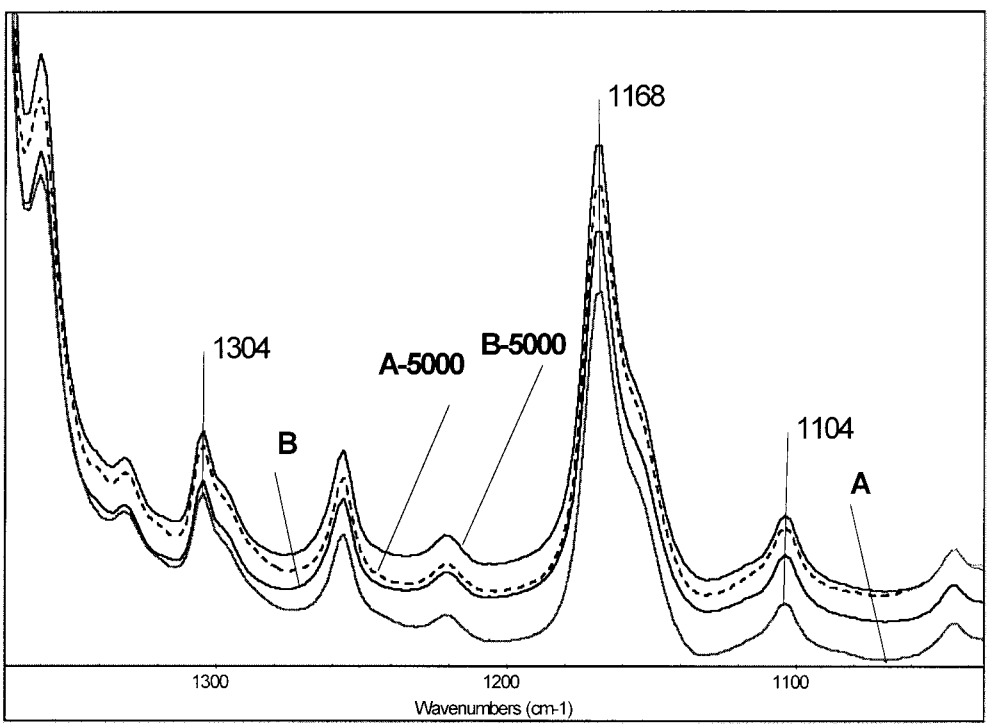

Figure 3 FTIR spectra of samples A and B exposed to artificial aging in the spectral range 1025–1380 cm^{-1}.

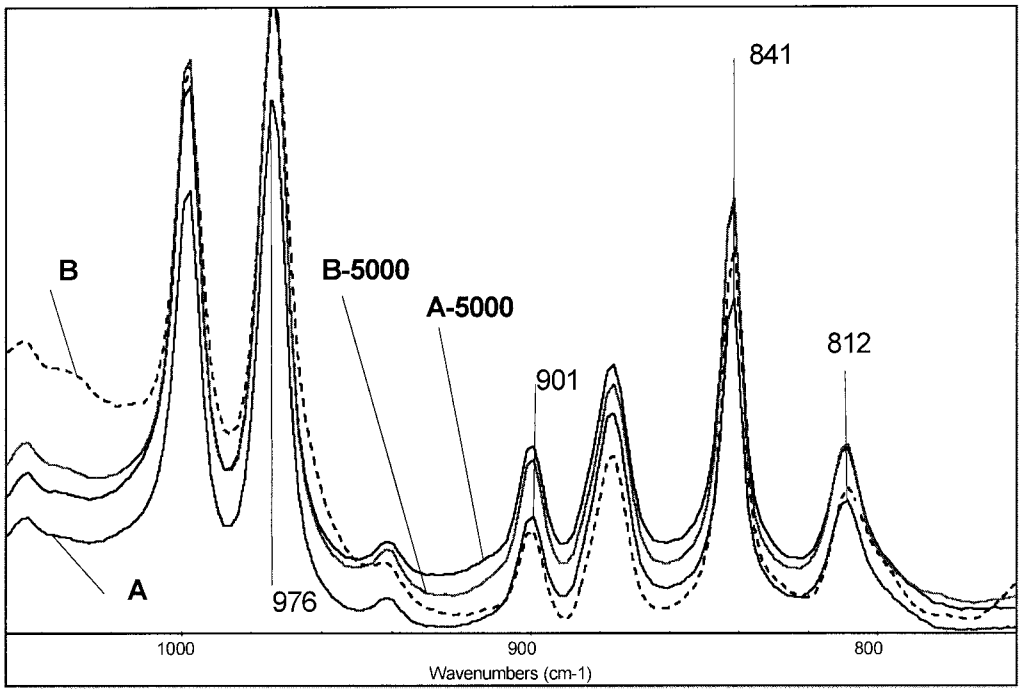

Figure 4 FTIR spectra of samples A and B exposed to artificial aging in the spectral range 750–1050 cm^{-1}. Bands marked with arrows are related to large spectral changes.

Comparing samples C and A (Fig. 5), which only differed in the pigment used and the type of aging, we can observe that natural aging is far more aggressive than artificial aging.

The formation of ether groups related to the 1168-cm^{-1} band (Figs. 1 and 3) is not clear in the artificially aged samples. This difference in the evolution of these groups must be influenced by parameters difficult to reproduce in artificial aging in a xenon test chamber (e.g., sudden changes of temperature and humidity, rain, and sea proximity). Furthermore, it is also difficult to reproduce the interactions of these parameters with the pigment used and the ability to react at high temperatures, mainly with sulfurous compounds[10] arising from pollution.

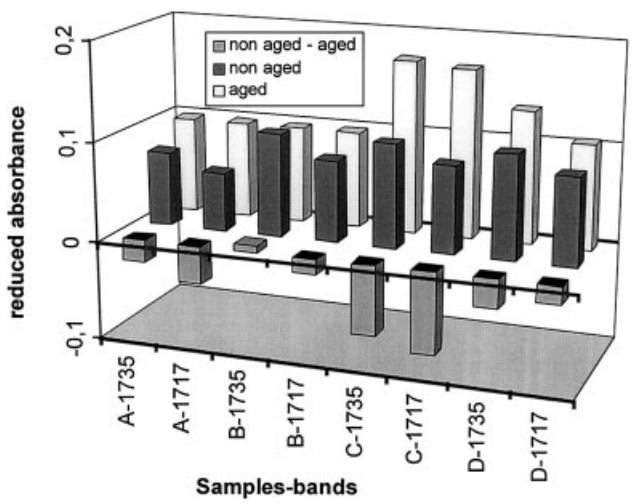

Figure 5 Reduced absorbance results of spectral bands associated with the carbonyl group in all aged samples.

There are several bands related to the double bonds. The one that can best help to define the evolution of the aging process is the 1650-cm^{-1} band, associated with the stretching vibrations of —C═C—.[11] The tendency of this band to diminish in the aged samples, as shown in Table II, is similar in all samples. Nevertheless, it is remarkable that samples artificially aged presented a decrease of 46%; compare this to 33% for the naturally aged ones. The double bonds are generated in the first steps of the aging process, reacting subsequently to produce branching, crosslinking, or both.

The samples exposed to natural aging had a lower percentage of double bonds but higher crosslinking. That is reflected in the configurational changes shown by the evolution of the main bands associated with the tacticity of PP (976, 901, and 812 cm^{-1})[11] in Figures 2 and 4.

The decline of every band, shown in Figure 6, occurred for all (naturally or artificially) aged samples. The spectral band most sensitive to the changes in the configuration order is the 976-cm^{-1} band, associated with ν(CC) in the chain and with $\gamma_r(CH_3)$.

Likewise, the tendency of the methyl (1378 cm^{-1}) and methylene (1460 cm^{-1}) groups to diminish was observed in all samples and in both aging processes. The results are given in Figure 7, which shows the evolution of the 1460- and 1378-cm^{-1} bands. The

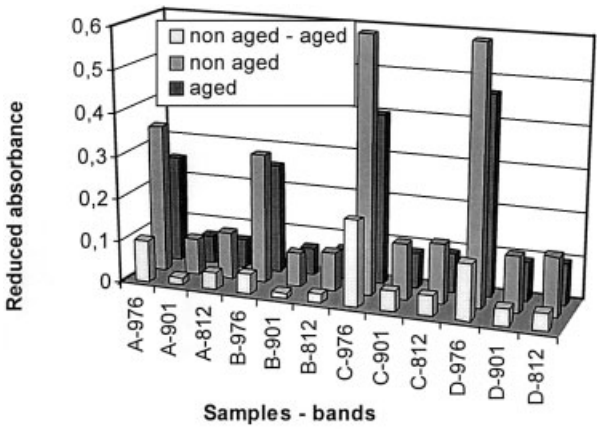

Figure 6 Reduced absorbance corresponding to spectral bands associated with configurational isomerism (976, 901, and 812 cm^{-1}) for all aged samples.

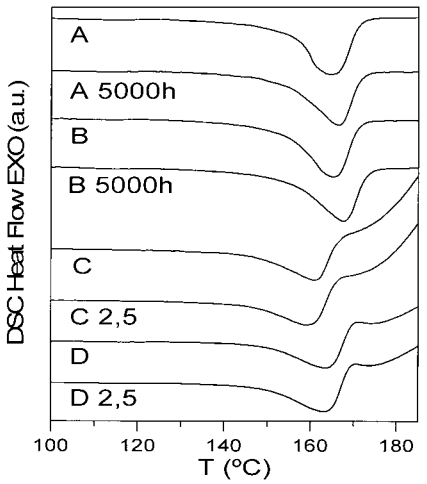

Figure 8 DSC curves corresponding to newly manufactured samples (A, B, C, and D) and the aged samples (A-5000, B-5000, C-2.5, and D-2.5).

greatest decrease occurred in the naturally aged ones (being more important in C than in D). The breaking of the group combined with the carbon in the natural aging process is widely accepted because this labile carbon easily becomes a free radical through elimination reactions[12,13] when ultraviolet radiation is present. Moreover, in most of the degradation processes of polyolefins, there is a decrease in the number of methylene groups. These phenomena help to confirm that macromolecular chains suffer homolytic and heterolytic breakage.[14] In this work, as shown in the results listed in Table II and Figure 7, a methylene decrease was also detected.

A chain break leads to the generation of terminal methyl groups, of which an increase would be expected, but our data revealed a decrease. This apparent contradiction is due to the fact that the number of methyl groups generated by chain scission is lower than the number of methyl groups that disappear in the formation of free radicals in tertiary carbons. The radicals generated present a high reactivity and provoke the rapid formation of nonsaturated bonds, which act as precursors in the formation of branching and crosslinking processes.

This transformation in the configurational order also appeared in samples A and B, although it was always present as a minor change.

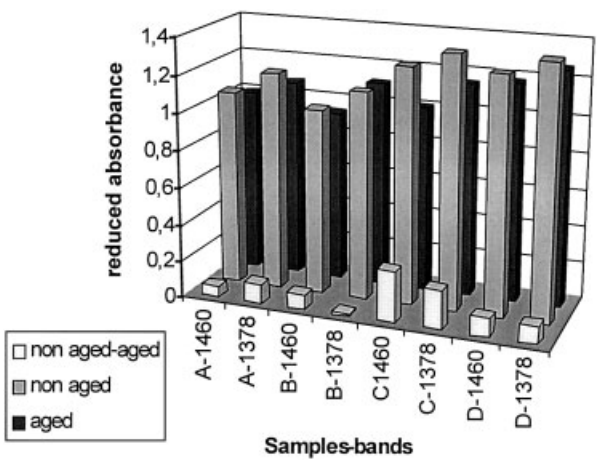

Figure 7 Reduced absorbance corresponding to spectral bands associated with methyl and methylene groups (1460 and 1378 cm^{-1}) for all aged samples.

Comparison of natural and artificial aging by DSC and SEM

Figure 8 shows the DSC thermograms of the samples, and Table III shows the characteristic thermal parameters of the melting and degradation processes.

In the calorimetric study performed by DSC (heating up to 600°C), several processes associated with melting and thermal decomposition (beginning after fusion) were detected. As shown in Table III, the decomposition process of the naturally aged samples (C and D) began at lower temperatures than in other samples. The difference between the melting onset temperature (T_o) for the decomposition process of ar-

TABLE III
Characteristics of Melting and Thermal Decomposition Processes

	Melting			Decomposition
Sample	T_o (°C)	T_p (°C)	ΔH (J/g)	T_o (°C)
A	155.0	164.5	81.2	193.5
A-5000	154.1	166.6	69.4	192.0
B	153.7	165.2	75.0	193.1
B-5000	154.9	167.3	72.1	191.2
C	154.1	166.1	73.6	193.8
C-2.5	149.5	161.5	43.6	166.7
D	153.9	166.3	84.4	193.9
D-2.5	150.0	164.0	55.0	169.8

tificially aged samples A and B and the nonaged samples was as low as 1–2°C, whereas the difference was greater for C and D samples (natural aging), being as high as 25–27°C. These differences also existed in the melting peak temperature (T_p) for the melting process. The decrease in the decomposition and melting temperatures is associated with shorter polymeric chains and a lower thermal stability of the material.

In the naturally aged samples (C and D), the melting enthalpy presented a clear decrease (ca. 40%) in comparison with the nonaged ones (Table III). The enthalpy decrease was intrinsically associated with a loss of the crystalline fraction of the copolymer, as previously shown by FTIR.

The calorimetric changes detected in the artificially aged samples (A and B) were lower than those observed in naturally aged ones. The melting enthalpy (ΔH) diminished by about 14% in the A samples and by about 4% in the B samples.

Previous studies on the crystallization kinetics of samples A and B led to the conclusion that these processes may be very sensitive to the presence of additives.[15,16] These results are confirmed in this work through the spectrophotometric and calorimetric studies. Nevertheless, in samples C and D, natural aging produced modifications of a larger magnitude than the use of different additives did.

The superficial morphology of aged samples depends on the type of aging. The surface of the samples aged by weather presented a scale structure, whereas the artificially aged surfaces preserved the original morphology, with the exception of several modified zones.

Another difference was detected when the samples were subjected to a thermal treatment followed by cooling to the crystallization temperature. The structure after the solidification process became porous (Fig. 9, top). Samples A and B, newly manufactured or after aging, presented similar morphologies, without preferential orientations, but the crystallization of samples C and D produced a micelle distribution (Fig. 9, bottom). This difference in behavior is related more to the presence of different additives than to degradation. Additive particles can act as nucleation centers of heterogeneous degradation. It appears that macroscopic structure modifications produced by natural and artificial degradation occur on the surface because an analysis of the internal areas of several broken samples did not show any differences between aged and nonaged samples.

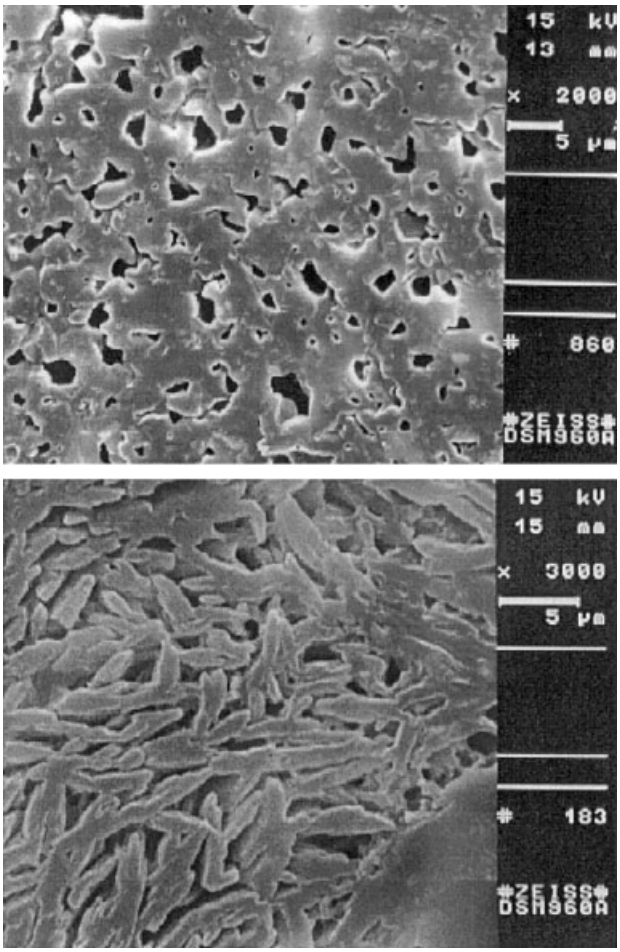

Figure 9 Micrographs corresponding to B-5000 artificial aging (top) and C-2.5 natural aging (bottom).

CONCLUSIONS

From the results obtained, it can be stated that natural aging produces configurational and conformational changes of a higher order than artificial aging. Oxidative processes are present in both kinds of aging. The main changes are the formation of carbonyl groups, the scission of hydrocarbonated chains, the formation of free radicals in tertiary carbons, and the initial formation of nonsaturated bonds followed by the progressive participation of these bonds in branching and crosslinking reactions.

The differences in behavior between the samples subjected to the same type of aging could be attributed to the presence of different commercial additives. For sample C, the combination of three types of antioxidants led to a synergistic effect that improved its stability against natural aging. Also, the catalytic effect of some colorants appeared in the results obtained.

DSC corroborated several of these results. The samples naturally aged showed a greater loss of crystallinity than those subjected to the xenon test. The melting enthalpy diminished by about 40% in the naturally aged samples and by only about 14% in the artificially aged samples.

The morphology obtained during the crystallization process was clearly different in samples subjected to both types of aging. This fact could be attributed to the additives used and to the differences between the aging processes.

The intended equivalence between the two types of aging processes has to be reviewed because the heterogeneous conditions in which natural aging occurs (e.g., environment, salinity content, rain, and pollution) produce a greater and more extensive effect than those of the xenon test.

References

1. Kaczmarek, H. Polymer 1996, 37, 189.
2. Carrasco, F.; Pagès, P.; Pascual, S.; Colom, X. Eur Polym J 2001, 37, 1457.
3. Colom, X.; García, T.; Suñol, J. J.; Saurina, J.; Carrasco, F. J Non-Cryst Solids 2001, 287, 308.
4. Esposito, L.; Koening, J. L. In Applications of Fourier Transform Infrared in Synthetic Polymers and Biological Macromolecules; Ferraro, J. R.; Basile, L. J., Eds.; Academic: New York, 1978; Vol. 1, Chapter 2.
5. Caykara, T.; Guven, O. Polym Degrad Stab 1999, 65, 225.
6. Chiantore, O.; Trossarelli, L.; Lazzari, M. Polymer 2000, 41, 1657.
7. Irusta, L.; Fernández-Berridi, M. J. Polymer 1999, 40, 4821.
8. EN 13206:2001; Annex A, Point 8.10.
9. Romeu, J.; Pagès, P.; Carrasco, F. Rev Plást Mod 1997, 74, 255.
10. Schnabel, W. Polymer Degradation Principles and Practical Applications; Hanser: New York, 1981.
11. Bower, D. I.; Maddams, W. F. The Vibrational Spectroscopy of Polymers; Cambridge University Press: Cambridge, England, 1989.
12. Vollhardt, C. Organic Chemistry; Freeman: New York, 1987.
13. Linstromberg, W. W. Organic Chemistry: A Brief Course; Heath: Lexington, MA, 1979.
14. Pagès, P.; Carrasco, F.; Saurina, J.; Colom, X. J Appl Polym Sci 1996, 60, 153.
15. Suñol, J. J.; Saurina, J.; Berlanga, R.; Herreros, Pagès, P.; Carrasco, F. J Therm Anal Calorim 1999, 55, 57.
16. Suñol, J. J.; Saurina, J.; Pagès, P.; Carrasco, F. J Appl Polym Sci 2000, 77, 1269.